

EUROPEAN ORGANIZATION FOR NUCLEAR RESEARCH (CERN)



CERN-PH-EP-2012-237

LHCb-PAPER-2012-015

June 5, 2018

Measurement of the fraction of $\Upsilon(1S)$ originating from $\chi_b(1P)$ decays in pp collisions at $\sqrt{s} = 7 \text{ TeV}$

The LHCb collaboration[†]

Abstract

The production of $\chi_b(1P)$ mesons in pp collisions at a centre-of-mass energy of 7 TeV is studied using 32 pb^{-1} of data collected with the LHCb detector. The $\chi_b(1P)$ mesons are reconstructed in the decay mode $\chi_b(1P) \rightarrow \Upsilon(1S)\gamma \rightarrow \mu^+\mu^-\gamma$. The fraction of $\Upsilon(1S)$ originating from $\chi_b(1P)$ decays in the $\Upsilon(1S)$ transverse momentum range $6 < p_{\text{T}}^{\Upsilon(1S)} < 15 \text{ GeV}/c$ and rapidity range $2.0 < y^{\Upsilon(1S)} < 4.5$ is measured to be $(20.7 \pm 5.7 \pm 2.1^{+2.7}_{-5.4})\%$, where the first uncertainty is statistical, the second is systematic and the last gives the range of the result due to the unknown $\Upsilon(1S)$ and $\chi_b(1P)$ polarizations.

Submitted to JHEP

[†]Authors are listed on the following pages.

LHCb collaboration

R. Aaij³⁸, C. Abellan Beteta^{33,n}, A. Adametz¹¹, B. Adeua³⁴, M. Adinolfi⁴³, C. Adrover⁶, A. Affolder⁴⁹, Z. Ajaltouni⁵, J. Albrecht³⁵, F. Alessio³⁵, M. Alexander⁴⁸, S. Ali³⁸, G. Alkhazov²⁷, P. Alvarez Cartelle³⁴, A.A. Alves Jr²², S. Amato², Y. Amhis³⁶, J. Anderson³⁷, R.B. Appleby⁵¹, O. Aquines Gutierrez¹⁰, F. Archilli^{18,35}, A. Artamonov³², M. Artuso^{53,35}, E. Aslanides⁶, G. Auriemma^{22,m}, S. Bachmann¹¹, J.J. Back⁴⁵, V. Balagura^{28,35}, W. Baldini¹⁶, R.J. Barlow⁵¹, C. Barschel³⁵, S. Barsuk⁷, W. Barter⁴⁴, A. Bates⁴⁸, C. Bauer¹⁰, Th. Bauer³⁸, A. Bay³⁶, J. Beddow⁴⁸, I. Bediaga¹, S. Belogurov²⁸, K. Belous³², I. Belyaev²⁸, E. Ben-Haim⁸, M. Benayoun⁸, G. Bencivenni¹⁸, S. Benson⁴⁷, J. Benton⁴³, R. Bernet³⁷, M.-O. Bettler¹⁷, M. van Beuzekom³⁸, A. Bien¹¹, S. Bifani¹², T. Bird⁵¹, A. Bizzeti^{17,h}, P.M. Bjørnstad⁵¹, T. Blake³⁵, F. Blanc³⁶, C. Blanks⁵⁰, J. Blouw¹¹, S. Blusk⁵³, A. Bobrov³¹, V. Bocci²², A. Bondar³¹, N. Bondar²⁷, W. Bonivento¹⁵, S. Borghi^{48,51}, A. Borgia⁵³, T.J.V. Bowcock⁴⁹, C. Bozzi¹⁶, T. Brambach⁹, J. van den Brand³⁹, J. Bressieux³⁶, D. Brett⁵¹, M. Britsch¹⁰, T. Britton⁵³, N.H. Brook⁴³, H. Brown⁴⁹, A. Büchler-Germann³⁷, I. Burducea²⁶, A. Bursche³⁷, J. Buytaert³⁵, S. Cadeddu¹⁵, O. Callot⁷, M. Calvi^{20,j}, M. Calvo Gomez^{33,n}, A. Camboni³³, P. Campana^{18,35}, A. Carbone¹⁴, G. Carboni^{21,k}, R. Cardinale^{19,i,35}, A. Cardini¹⁵, L. Carson⁵⁰, K. Carvalho Akiba², G. Casse⁴⁹, M. Cattaneo³⁵, Ch. Cauet⁹, M. Charles⁵², Ph. Charpentier³⁵, P. Chen^{3,36}, N. Chiapolini³⁷, M. Chrzaszcz²³, K. Ciba³⁵, X. Cid Vidal³⁴, G. Ciezarek⁵⁰, P.E.L. Clarke⁴⁷, M. Clemencic³⁵, H.V. Cliff⁴⁴, J. Closier³⁵, C. Coca²⁶, V. Coco³⁸, J. Cogan⁶, E. Cogneras⁵, P. Collins³⁵, A. Comerma-Montells³³, A. Contu⁵², A. Cook⁴³, M. Coombes⁴³, G. Corti³⁵, B. Couturier³⁵, G.A. Cowan³⁶, D. Craik⁴⁵, R. Currie⁴⁷, C. D'Ambrosio³⁵, P. David⁸, P.N.Y. David³⁸, I. De Bonis⁴, K. De Bruyn³⁸, S. De Capua^{21,k}, M. De Cian³⁷, J.M. De Miranda¹, L. De Paula², P. De Simone¹⁸, D. Decamp⁴, M. Deckenhoff⁹, H. Degaudenzi^{36,35}, L. Del Buono⁸, C. Deplano¹⁵, D. Derkach^{14,35}, O. Deschamps⁵, F. Dettori³⁹, J. Dickens⁴⁴, H. Dijkstra³⁵, P. Diniz Batista¹, F. Domingo Bonal^{33,n}, S. Donleavy⁴⁹, F. Dordei¹¹, A. Dosil Suárez³⁴, D. Dossett⁴⁵, A. Dovbnya⁴⁰, F. Dupertuis³⁶, R. Dzhelyadin³², A. Dziurda²³, A. Dzyuba²⁷, S. Easo⁴⁶, U. Egede⁵⁰, V. Egorychev²⁸, S. Eidelman³¹, D. van Eijk³⁸, F. Eisele¹¹, S. Eisenhardt⁴⁷, R. Ekelhof⁹, L. Eklund⁴⁸, I. El Rifai⁵, Ch. Elsasser³⁷, D. Elsby⁴², D. Esperante Pereira³⁴, A. Falabella^{16,e,14}, C. Färber¹¹, G. Fardell⁴⁷, C. Farinelli³⁸, S. Farry¹², V. Fave³⁶, V. Fernandez Albor³⁴, F. Ferreira Rodrigues¹, M. Ferro-Luzzi³⁵, S. Filippov³⁰, C. Fitzpatrick⁴⁷, M. Fontana¹⁰, F. Fontanelli^{19,i}, R. Forty³⁵, O. Francisco², M. Frank³⁵, C. Frei³⁵, M. Frosini^{17,f}, S. Furcas²⁰, A. Gallas Torreira³⁴, D. Galli^{14,c}, M. Gandelman², P. Gandini⁵², Y. Gao³, J-C. Garnier³⁵, J. Garofoli⁵³, J. Garra Tico⁴⁴, L. Garrido³³, D. Gascon³³, C. Gaspar³⁵, R. Gauld⁵², N. Gauvin³⁶, E. Gersabeck¹¹, M. Gersabeck³⁵, T. Gershon^{45,35}, Ph. Ghez⁴, V. Gibson⁴⁴, V.V. Gligorov³⁵, C. Göbel⁵⁴, D. Golubkov²⁸, A. Golutvin^{50,28,35}, A. Gomes², H. Gordon⁵², M. Grabalosa Gándara³³, R. Graciani Diaz³³, L.A. Granado Cardoso³⁵, E. Graugés³³, G. Graziani¹⁷, A. Grecu²⁶, E. Greening⁵², S. Gregson⁴⁴, O. Grünberg⁵⁵, B. Gui⁵³, E. Gushchin³⁰, Yu. Guz³², T. Gys³⁵, C. Hadjivasiliou⁵³, G. Haefeli³⁶, C. Haen³⁵, S.C. Haines⁴⁴, T. Hampson⁴³, S. Hansmann-Menzemer¹¹, N. Harnew⁵², S.T. Harnew⁴³, J. Harrison⁵¹, P.F. Harrison⁴⁵, T. Hartmann⁵⁵, J. He⁷, V. Heijne³⁸, K. Hennessy⁴⁹, P. Henrard⁵, J.A. Hernando Morata³⁴, E. van Herwijnen³⁵, E. Hicks⁴⁹, M. Hoballah⁵, P. Hopchev⁴, W. Hulsbergen³⁸, P. Hunt⁵², T. Huse⁴⁹, R.S. Huston¹², D. Hutchcroft⁴⁹, D. Hynds⁴⁸, V. Iakovenko⁴¹, P. Ilten¹², J. Imong⁴³, R. Jacobsson³⁵, A. Jaeger¹¹, M. Jahjah Hussein⁵, E. Jans³⁸, F. Jansen³⁸, P. Jaton³⁶, B. Jean-Marie⁷, F. Jing³, M. John⁵², D. Johnson⁵²,

C.R. Jones⁴⁴, B. Jost³⁵, M. Kaballo⁹, S. Kandybei⁴⁰, M. Karacson³⁵, T.M. Karbach⁹,
 J. Keaveney¹², I.R. Kenyon⁴², U. Kerzel³⁵, T. Ketel³⁹, A. Keune³⁶, B. Khanji⁶, Y.M. Kim⁴⁷,
 M. Knecht³⁶, O. Kochebina⁷, I. Komarov²⁹, R.F. Koopman³⁹, P. Koppenburg³⁸, M. Korolev²⁹,
 A. Kozlinskiy³⁸, L. Kravchuk³⁰, K. Kreplin¹¹, M. Kreps⁴⁵, G. Krocker¹¹, P. Krovovny³¹,
 F. Kruse⁹, M. Kucharczyk^{20,23,35,j}, V. Kudryavtsev³¹, T. Kvaratskheliya^{28,35}, V.N. La Thi³⁶,
 D. Lacarrere³⁵, G. Lafferty⁵¹, A. Lai¹⁵, D. Lambert⁴⁷, R.W. Lambert³⁹, E. Lanciotti³⁵,
 G. Lanfranchi¹⁸, C. Langenbruch³⁵, T. Latham⁴⁵, C. Lazzeroni⁴², R. Le Gac⁶,
 J. van Leerdam³⁸, J.-P. Lees⁴, R. Lefèvre⁵, A. Leflat^{29,35}, J. Lefrançois⁷, O. Leroy⁶,
 T. Lesiak²³, L. Li³, Y. Li³, L. Li Gioi⁵, M. Lieng⁹, M. Liles⁴⁹, R. Lindner³⁵, C. Linn¹¹, B. Liu³,
 G. Liu³⁵, J. von Loeben²⁰, J.H. Lopes², E. Lopez Asamar³³, N. Lopez-March³⁶, H. Lu³,
 J. Luisier³⁶, A. Mac Raighne⁴⁸, F. Machefert⁷, I.V. Machikhiliyan^{4,28}, F. Maciuc¹⁰,
 O. Maev^{27,35}, J. Magnin¹, S. Malde⁵², R.M.D. Mamunur³⁵, G. Manca^{15,d}, G. Mancinelli⁶,
 N. Mangiafave⁴⁴, U. Marconi¹⁴, R. Märki³⁶, J. Marks¹¹, G. Martellotti²², A. Martens⁸,
 L. Martin⁵², A. Martín Sánchez⁷, M. Martinelli³⁸, D. Martinez Santos³⁵, A. Massafferri¹,
 Z. Mathe¹², C. Matteuzzi²⁰, M. Matveev²⁷, E. Maurice⁶, A. Mazurov^{16,30,35}, J. McCarthy⁴²,
 G. McGregor⁵¹, R. McNulty¹², M. Meissner¹¹, M. Merk³⁸, J. Merkel⁹, D.A. Milanes¹³,
 M.-N. Minard⁴, J. Molina Rodriguez⁵⁴, S. Monteil⁵, D. Moran¹², P. Morawski²³,
 R. Mountain⁵³, I. Mous³⁸, F. Muheim⁴⁷, K. Müller³⁷, R. Muresan²⁶, B. Muryn²⁴, B. Muster³⁶,
 J. Mylroie-Smith⁴⁹, P. Naik⁴³, T. Nakada³⁶, R. Nandakumar⁴⁶, I. Nasteva¹, M. Needham⁴⁷,
 N. Neufeld³⁵, A.D. Nguyen³⁶, C. Nguyen-Mau^{36,o}, M. Nicol⁷, V. Niess⁵, N. Nikitin²⁹,
 T. Nikodem¹¹, A. Nomerotski^{52,35}, A. Novoselov³², A. Oblakowska-Mucha²⁴, V. Obraztsov³²,
 S. Oggero³⁸, S. Ogilvy⁴⁸, O. Okhrimenko⁴¹, R. Oldeman^{15,d,35}, M. Orlandea²⁶,
 J.M. Otalora Goicochea², P. Owen⁵⁰, B.K. Pal⁵³, A. Palano^{13,b}, M. Palutan¹⁸, J. Panman³⁵,
 A. Papanestis⁴⁶, M. Pappagallo⁴⁸, C. Parkes⁵¹, C.J. Parkinson⁵⁰, G. Passaleva¹⁷, G.D. Patel⁴⁹,
 M. Patel⁵⁰, G.N. Patrick⁴⁶, C. Patrignani^{19,i}, C. Pavel-Nicorescu²⁶, A. Pazos Alvarez³⁴,
 A. Pellegrino³⁸, G. Penso^{22,l}, M. Pepe Altarelli³⁵, S. Perazzini^{14,c}, D.L. Perego^{20,j},
 E. Perez Trigo³⁴, A. Pérez-Calero Yzquierdo³³, P. Perret⁵, M. Perrin-Terrin⁶, G. Pessina²⁰,
 A. Petrolini^{19,i}, A. Phan⁵³, E. Picatoste Olloqui³³, B. Pie Valls³³, B. Pietrzyk⁴, T. Pilarčík⁴⁵,
 D. Pinci²², S. Playfer⁴⁷, M. Plo Casasus³⁴, F. Polci⁸, G. Polok²³, A. Poluektov^{45,31},
 E. Polycarpo², D. Popov¹⁰, B. Popovici²⁶, C. Potterat³³, A. Powell⁵², J. Prisciandaro³⁶,
 V. Pugatch⁴¹, A. Puig Navarro³³, W. Qian⁵³, J.H. Rademacker⁴³, B. Rakotomiaramanana³⁶,
 M.S. Rangel², I. Raniuk⁴⁰, N. Rauschmayr³⁵, G. Raven³⁹, S. Redford⁵², M.M. Reid⁴⁵,
 A.C. dos Reis¹, S. Ricciardi⁴⁶, A. Richards⁵⁰, K. Rinnert⁴⁹, D.A. Roa Romero⁵, P. Robbe⁷,
 E. Rodrigues^{48,51}, F. Rodrigues², P. Rodriguez Perez³⁴, G.J. Rogers⁴⁴, S. Roiser³⁵,
 V. Romanovsky³², A. Romero Vidal³⁴, M. Rosello^{33,n}, J. Rouvinet³⁶, T. Ruf³⁵, H. Ruiz³³,
 G. Sabatino^{21,k}, J.J. Saborido Silva³⁴, N. Sagidova²⁷, P. Sail⁴⁸, B. Saitta^{15,d}, C. Salzmann³⁷,
 B. Sanmartin Sedes³⁴, M. Sannino^{19,i}, R. Santacesaria²², C. Santamarina Rios³⁴,
 R. Santinelli³⁵, E. Santovetti^{21,k}, M. Sapunov⁶, A. Sarti^{18,l}, C. Satriano^{22,m}, A. Satta²¹,
 M. Savrie^{16,e}, D. Savrina²⁸, P. Schaack⁵⁰, M. Schiller³⁹, H. Schindler³⁵, S. Schleich⁹,
 M. Schlupp⁹, M. Schmelling¹⁰, B. Schmidt³⁵, O. Schneider³⁶, A. Schopper³⁵, M.-H. Schune⁷,
 R. Schwemmer³⁵, B. Sciascia¹⁸, A. Sciubba^{18,l}, M. Seco³⁴, A. Semennikov²⁸, K. Senderowska²⁴,
 I. Sepp⁵⁰, N. Serra³⁷, J. Serrano⁶, P. Seyfert¹¹, M. Shapkin³², I. Shapoval^{40,35}, P. Shatalov²⁸,
 Y. Shcheglov²⁷, T. Shears⁴⁹, L. Shekhtman³¹, O. Shevchenko⁴⁰, V. Shevchenko²⁸, A. Shires⁵⁰,
 R. Silva Coutinho⁴⁵, T. Skwarnicki⁵³, N.A. Smith⁴⁹, E. Smith^{52,46}, M. Smith⁵¹, K. Sobczak⁵,
 F.J.P. Soler⁴⁸, A. Solomin⁴³, F. Soomro^{18,35}, D. Souza⁴³, B. Souza De Paula², B. Spaan⁹,
 A. Sparkes⁴⁷, P. Spradlin⁴⁸, F. Stagni³⁵, S. Stahl¹¹, O. Steinkamp³⁷, S. Stoica²⁶, S. Stone^{53,35},

B. Storaci³⁸, M. Straticiuc²⁶, U. Straumann³⁷, V.K. Subbiah³⁵, S. Swientek⁹,
M. Szczekowski²⁵, P. Szczypka³⁶, T. Szumlak²⁴, S. T'Jampens⁴, M. Teklishyn⁷,
E. Teodorescu²⁶, F. Teubert³⁵, C. Thomas⁵², E. Thomas³⁵, J. van Tilburg¹¹, V. Tisserand⁴,
M. Tobin³⁷, S. Tolk³⁹, S. Topp-Joergensen⁵², N. Torr⁵², E. Tournefier^{4,50}, S. Tourneur³⁶,
M.T. Tran³⁶, A. Tsaregorodtsev⁶, N. Tuning³⁸, M. Ubeda Garcia³⁵, A. Ukleja²⁵, U. Uwer¹¹,
V. Vagnoni¹⁴, G. Valenti¹⁴, R. Vazquez Gomez³³, P. Vazquez Regueiro³⁴, S. Vecchi¹⁶,
J.J. Velthuis⁴³, M. Veltri^{17,g}, G. Veneziano³⁶, M. Vesterinen³⁵, B. Viaud⁷, I. Videau⁷,
D. Vieira², X. Vilasis-Cardona^{33,n}, J. Visniakov³⁴, A. Vollhardt³⁷, D. Volyansky¹⁰,
D. Voong⁴³, A. Vorobyev²⁷, V. Vorobyev³¹, C. Voß⁵⁵, H. Voss¹⁰, R. Waldi⁵⁵, R. Wallace¹²,
S. Wandernoth¹¹, J. Wang⁵³, D.R. Ward⁴⁴, N.K. Watson⁴², A.D. Webber⁵¹, D. Websdale⁵⁰,
M. Whitehead⁴⁵, J. Wicht³⁵, D. Wiedner¹¹, L. Wiggers³⁸, G. Wilkinson⁵², M.P. Williams^{45,46},
M. Williams⁵⁰, F.F. Wilson⁴⁶, J. Wishahi⁹, M. Witek²³, W. Witzeling³⁵, S.A. Wotton⁴⁴,
S. Wright⁴⁴, S. Wu³, K. Wyllie³⁵, Y. Xie⁴⁷, F. Xing⁵², Z. Xing⁵³, Z. Yang³, R. Young⁴⁷,
X. Yuan³, O. Yushchenko³², M. Zangoli¹⁴, M. Zavertyaev^{10,a}, F. Zhang³, L. Zhang⁵³,
W.C. Zhang¹², Y. Zhang³, A. Zhelezov¹¹, L. Zhong³, A. Zvyagin³⁵.

¹*Centro Brasileiro de Pesquisas Físicas (CBPF), Rio de Janeiro, Brazil*

²*Universidade Federal do Rio de Janeiro (UFRJ), Rio de Janeiro, Brazil*

³*Center for High Energy Physics, Tsinghua University, Beijing, China*

⁴*LAPP, Université de Savoie, CNRS/IN2P3, Annecy-Le-Vieux, France*

⁵*Clermont Université, Université Blaise Pascal, CNRS/IN2P3, LPC, Clermont-Ferrand, France*

⁶*CPPM, Aix-Marseille Université, CNRS/IN2P3, Marseille, France*

⁷*LAL, Université Paris-Sud, CNRS/IN2P3, Orsay, France*

⁸*LPNHE, Université Pierre et Marie Curie, Université Paris Diderot, CNRS/IN2P3, Paris, France*

⁹*Fakultät Physik, Technische Universität Dortmund, Dortmund, Germany*

¹⁰*Max-Planck-Institut für Kernphysik (MPIK), Heidelberg, Germany*

¹¹*Physikalisches Institut, Ruprecht-Karls-Universität Heidelberg, Heidelberg, Germany*

¹²*School of Physics, University College Dublin, Dublin, Ireland*

¹³*Sezione INFN di Bari, Bari, Italy*

¹⁴*Sezione INFN di Bologna, Bologna, Italy*

¹⁵*Sezione INFN di Cagliari, Cagliari, Italy*

¹⁶*Sezione INFN di Ferrara, Ferrara, Italy*

¹⁷*Sezione INFN di Firenze, Firenze, Italy*

¹⁸*Laboratori Nazionali dell'INFN di Frascati, Frascati, Italy*

¹⁹*Sezione INFN di Genova, Genova, Italy*

²⁰*Sezione INFN di Milano Bicocca, Milano, Italy*

²¹*Sezione INFN di Roma Tor Vergata, Roma, Italy*

²²*Sezione INFN di Roma La Sapienza, Roma, Italy*

²³*Henryk Niewodniczanski Institute of Nuclear Physics Polish Academy of Sciences, Kraków, Poland*

²⁴*AGH University of Science and Technology, Kraków, Poland*

²⁵*Soltan Institute for Nuclear Studies, Warsaw, Poland*

²⁶*Horia Hulubei National Institute of Physics and Nuclear Engineering, Bucharest-Magurele, Romania*

²⁷*Petersburg Nuclear Physics Institute (PNPI), Gatchina, Russia*

²⁸*Institute of Theoretical and Experimental Physics (ITEP), Moscow, Russia*

²⁹*Institute of Nuclear Physics, Moscow State University (SINP MSU), Moscow, Russia*

³⁰*Institute for Nuclear Research of the Russian Academy of Sciences (INR RAN), Moscow, Russia*

³¹*Budker Institute of Nuclear Physics (SB RAS) and Novosibirsk State University, Novosibirsk, Russia*

³²*Institute for High Energy Physics (IHEP), Protvino, Russia*

³³*Universitat de Barcelona, Barcelona, Spain*

³⁴*Universidad de Santiago de Compostela, Santiago de Compostela, Spain*

- ³⁵European Organization for Nuclear Research (CERN), Geneva, Switzerland
³⁶Ecole Polytechnique Fédérale de Lausanne (EPFL), Lausanne, Switzerland
³⁷Physik-Institut, Universität Zürich, Zürich, Switzerland
³⁸Nikhef National Institute for Subatomic Physics, Amsterdam, The Netherlands
³⁹Nikhef National Institute for Subatomic Physics and VU University Amsterdam, Amsterdam, The Netherlands
⁴⁰NSC Kharkiv Institute of Physics and Technology (NSC KIPT), Kharkiv, Ukraine
⁴¹Institute for Nuclear Research of the National Academy of Sciences (KINR), Kyiv, Ukraine
⁴²University of Birmingham, Birmingham, United Kingdom
⁴³H.H. Wills Physics Laboratory, University of Bristol, Bristol, United Kingdom
⁴⁴Cavendish Laboratory, University of Cambridge, Cambridge, United Kingdom
⁴⁵Department of Physics, University of Warwick, Coventry, United Kingdom
⁴⁶STFC Rutherford Appleton Laboratory, Didcot, United Kingdom
⁴⁷School of Physics and Astronomy, University of Edinburgh, Edinburgh, United Kingdom
⁴⁸School of Physics and Astronomy, University of Glasgow, Glasgow, United Kingdom
⁴⁹Oliver Lodge Laboratory, University of Liverpool, Liverpool, United Kingdom
⁵⁰Imperial College London, London, United Kingdom
⁵¹School of Physics and Astronomy, University of Manchester, Manchester, United Kingdom
⁵²Department of Physics, University of Oxford, Oxford, United Kingdom
⁵³Syracuse University, Syracuse, NY, United States
⁵⁴Pontifícia Universidade Católica do Rio de Janeiro (PUC-Rio), Rio de Janeiro, Brazil, associated to ²
⁵⁵Institut für Physik, Universität Rostock, Rostock, Germany, associated to ¹¹
- ^aP.N. Lebedev Physical Institute, Russian Academy of Science (LPI RAS), Moscow, Russia
^bUniversità di Bari, Bari, Italy
^cUniversità di Bologna, Bologna, Italy
^dUniversità di Cagliari, Cagliari, Italy
^eUniversità di Ferrara, Ferrara, Italy
^fUniversità di Firenze, Firenze, Italy
^gUniversità di Urbino, Urbino, Italy
^hUniversità di Modena e Reggio Emilia, Modena, Italy
ⁱUniversità di Genova, Genova, Italy
^jUniversità di Milano Bicocca, Milano, Italy
^kUniversità di Roma Tor Vergata, Roma, Italy
^lUniversità di Roma La Sapienza, Roma, Italy
^mUniversità della Basilicata, Potenza, Italy
ⁿLIFAELS, La Salle, Universitat Ramon Llull, Barcelona, Spain
^oHanoi University of Science, Hanoi, Viet Nam

1 Introduction

The production of heavy quarkonium states at hadron colliders is a subject of experimental and theoretical interest [1]. The non-relativistic QCD (NRQCD) factorization approach has been developed to describe the inclusive production and decay of quarkonia [2]. The LHCb experiment has measured the production of inclusive $J/\psi \rightarrow \mu^+ \mu^-$ [3], $\psi(2S)$ [4] and $\Upsilon(nS) \rightarrow \mu^+ \mu^-$ ($n = 1, 2, 3$) [5] mesons in pp collisions as a function of the quarkonium transverse momentum p_T and rapidity y over the range $0 < p_T < 15 \text{ GeV}/c$ and $2.0 < y < 4.5$. A significant fraction of the cross-section for both J/ψ and $\Upsilon(nS)$ production is expected to be due to feed-down from higher quarkonium states. Understanding the size of this effect is important for the interpretation of the quarkonia cross-section and polarization data. A few experimental studies of hadroproduction of P -wave quarkonia have been reported. In the case of the χ_{cJ} states, with spin $J = 0, 1, 2$, measurements from the CDF [6, 7], HERA-B [8] and LHCb [9, 10] experiments exist, while χ_{bJ} related measurements have been reported by the CDF [11], ATLAS [12] and D0 [13] experiments.

This paper reports studies of the inclusive production of the P -wave $\chi_{bJ}(1P)$ states, collectively referred to as $\chi_b(1P)$ throughout the paper. The $\chi_b(1P)$ mesons are reconstructed through the radiative decay $\chi_b(1P) \rightarrow \Upsilon(1S)\gamma$ in the $\Upsilon(1S)$ rapidity and transverse momentum range $2.0 < y^{\Upsilon(1S)} < 4.5$ and $6 < p_T^{\Upsilon(1S)} < 15 \text{ GeV}/c$. The χ_{b2} and χ_{b1} states differ in mass by $20 \text{ MeV}/c^2$ and the χ_{b1} and χ_{b0} states by $33 \text{ MeV}/c^2$ [14]. Since these differences are comparable with the experimental resolution, the total fraction of $\Upsilon(1S)$ originating from $\chi_b(1P)$ decays is reported. The results presented here use a data sample collected at the LHC with the LHCb detector at a centre-of-mass energy of 7 TeV and correspond to an integrated luminosity of 32 pb^{-1} .

2 LHCb detector

The LHCb detector [15] is a single-arm forward spectrometer covering the pseudorapidity range $2 < \eta < 5$, designed for the study of particles containing b or c quarks. The detector includes a high precision tracking system consisting of a silicon-strip vertex detector surrounding the pp interaction region, a large-area silicon-strip detector located upstream of a dipole magnet with a bending power of about 4 Tm , and three stations of silicon-strip detectors and straw drift tubes placed downstream. The combined tracking system has a momentum resolution $\Delta p/p$ that varies from 0.4% at $5 \text{ GeV}/c$ to 0.6% at $100 \text{ GeV}/c$, and an impact parameter resolution of $20 \mu\text{m}$ for tracks with high transverse momentum (p_T). Charged hadrons are identified using two ring-imaging Cherenkov detectors. Photon, electron and hadron candidates are identified by a calorimeter system consisting of scintillating-pad and preshower detectors, an electromagnetic calorimeter and a hadronic calorimeter. Muons are identified by a system composed of alternating layers of iron and multiwire proportional chambers. The nominal detector performance for photons and muons is described in [15]. The processes of radiative transitions of $\chi_{cJ} \rightarrow J/\psi\gamma$, $J = 1, 2$ with similar kinematics of the photons are studied in [9, 10]. Another physical analysis which uses $\pi^0 \rightarrow \gamma\gamma$, $\eta \rightarrow \gamma\gamma$ and $\eta' \rightarrow \rho^0\gamma$ is available as [16].

The trigger consists of a hardware stage followed by a software stage which applies a full event reconstruction. The trigger used for this analysis selects a pair of oppositely-charged muon candidates, where either one of the muons has a $p_T > 1.8 \text{ GeV}/c$ or one of the pair has a $p_T > 0.56 \text{ GeV}/c$ and the other has a $p_T > 0.48 \text{ GeV}/c$. The invariant mass of the pair is required to be greater than $2.9 \text{ GeV}/c^2$. The photons are not used in the trigger decision.

For the simulation, pp collisions are generated using PYTHIA 6.4 [17] with a specific LHCb configuration [18]. Decays of hadronic particles are described by EVTGEN [19] in which final state radiation is generated using PHOTOS [20]. The interaction of the generated particles with the detector and its response are implemented using the GEANT4 toolkit [21] as described in Ref. [22]. The simulated signal events contain at least one $\Upsilon(1S) \rightarrow \mu^+ \mu^-$ decay with both muons in the LHCb acceptance. In this sample of simulated events the fraction of $\Upsilon(1S)$ mesons produced in $\chi_b(1P)$ decays is 47% and both the $\chi_b(1P)$ and $\Upsilon(1S)$ mesons are produced unpolarized.

3 Event selection

The reconstruction of the $\chi_b(1P)$ meson proceeds via the identification of an $\Upsilon(1S)$ meson combined with a reconstructed photon. The $\Upsilon(nS)$ candidates are formed from a pair of oppositely-charged tracks that are identified as muons. Each track is required to have a good track fit quality. The two muons are required to originate from a common vertex with a distance to the primary vertex less than 1 mm.

The invariant mass distribution of the $\mu^+ \mu^-$ candidates is shown in Fig. 1. It is modelled with the sum of three Crystal Ball functions [23], describing the $\Upsilon(1S)$, $\Upsilon(2S)$ and $\Upsilon(3S)$ signals, and an exponential function for the combinatorial background. The parameters of the Crystal Ball functions that describe the radiative tail of the $\Upsilon(1S)$, $\Upsilon(2S)$ and $\Upsilon(3S)$ mass distributions are fixed to the values $a = 2$ and $n = 1$ [5]. The measured $\Upsilon(1S)$ signal yield, mass and width are $N_{\Upsilon(1S)} = 39\,635 \pm 252$, $m_{\Upsilon(1S)} = 9449.2 \pm 0.4 \text{ MeV}/c^2$ and $\sigma_{\Upsilon(1S)} = 51.7 \pm 0.4 \text{ MeV}/c^2$, where the uncertainties are statistical only.

The $\Upsilon(1S)$ candidates with a $p_T^{\Upsilon(1S)} > 6 \text{ GeV}/c$ and a $\mu^+ \mu^-$ invariant mass in the range $9.36 - 9.56 \text{ GeV}/c^2$ are combined with photons to form $\chi_b(1P)$ candidates. The photons are required to have $p_T^\gamma > 0.6 \text{ GeV}/c$ and $\cos \theta_\gamma^* > 0$, where θ_γ^* is the angle of the photon direction in the centre-of-mass frame of the $\mu^+ \mu^- \gamma$ system with respect to the momentum of this system in the laboratory frame.

The $\chi_b(1P)$ signal peak observed in the distribution of the mass difference, $x = m(\mu^+ \mu^- \gamma) - m(\mu^+ \mu^-)$, is shown in Fig. 2 for the range $6 < p_T^{\Upsilon(1S)} < 15 \text{ GeV}/c$. It is modelled with an empirical function given by

$$\frac{dN}{dx} = A_1 \frac{1}{\sqrt{2\pi}\sigma} e^{-\frac{(x-\Delta M)^2}{2\sigma^2}} + A_2(x-x_0)^\alpha e^{-(c_1x+c_2x^2+c_3x^3)}, \quad (1)$$

where A_1 , ΔM , σ , A_2 , x_0 , α , c_1 , c_2 and c_3 are free parameters. The Gaussian function describes the signal and the second term models the background. The number of $\chi_b(1P)$

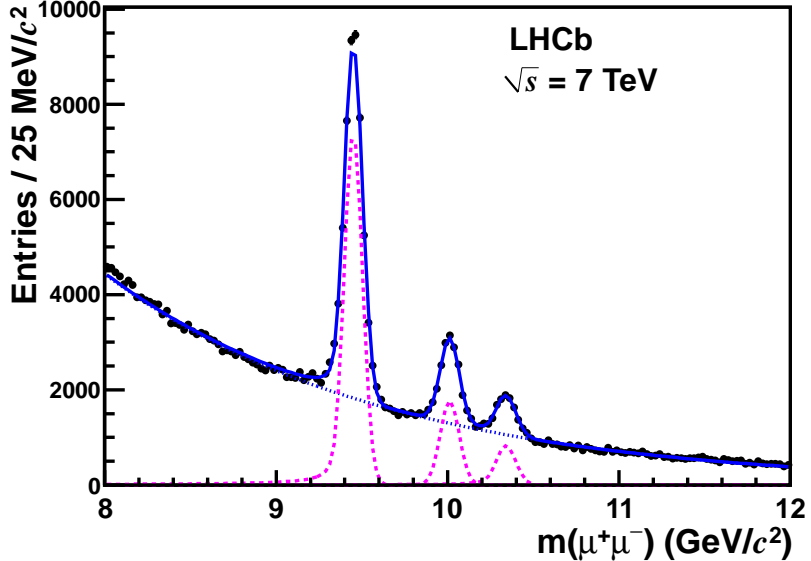


Figure 1: Distribution of the $\mu^+\mu^-$ mass for selected $\Upsilon(nS)$ candidates (black points), together with the result of the fit (solid blue curve), including the background (dotted blue curve) and the signal (dashed magenta curve) contributions.

signal decays obtained from the fit is 201 ± 55 . The mean value of the Gaussian function is $447 \pm 4 \text{ MeV}/c^2$ and its width is $19.0 \pm 4.2 \text{ MeV}/c^2$. The expected values of the mass differences for the three $\chi_{bJ}(1P)$ states are $\Delta M(\chi_{b2}) = 452 \text{ MeV}/c^2$, $\Delta M(\chi_{b1}) = 432 \text{ MeV}/c^2$ and $\Delta M(\chi_{b0}) = 399 \text{ MeV}/c^2$ [14]. The peak position in the data lies between $\Delta M(\chi_{b2})$ and $\Delta M(\chi_{b0})$ as expected for any mixture of $\chi_{bJ}(1P)$ states.

4 Fraction of $\Upsilon(1S)$ originating from $\chi_b(1P)$ decays

The fraction of $\Upsilon(1S)$ originating from $\chi_b(1P)$ decays is determined using the following assumptions. Firstly, all $\Upsilon(1S)$ originating from $\chi_b(1P)$ arise from the radiative decay $\chi_b(1P) \rightarrow \Upsilon(1S)\gamma$. Secondly, the total efficiency for $\Upsilon(1S) \rightarrow \mu^+\mu^-$ as a function of $p_T^{\Upsilon(1S)}$ is the same for directly produced $\Upsilon(1S)$ and for those from feed-down from $\chi_b(1P)$. The total efficiency includes trigger, detection, reconstruction and selection. Thirdly, the photon detection, reconstruction and selection are independent of the $\Upsilon(1S) \rightarrow \mu^+\mu^-$. Hence the total efficiency for $\chi_b(1P)$ is factorized as $\epsilon_{\text{tot}}(\chi_b) = \epsilon_{\text{cond}}(\chi_b) \cdot \epsilon_{\text{tot}}(\Upsilon)$, where $\epsilon_{\text{tot}}(\Upsilon)$ is the total efficiency for $\Upsilon(1S)$ and $\epsilon_{\text{cond}}(\chi_b)$ is the conditional efficiency for $\chi_b(1P)$ reconstruction and selection after the $\Upsilon(1S) \rightarrow \mu^+\mu^-$ candidate has been selected.

The second assumption is tested by comparing the $\Upsilon(1S)$ efficiencies obtained using simulated events for direct $\Upsilon(1S)$ and for $\Upsilon(1S)$ coming from decays of $\chi_b(1P)$ states. These efficiencies for each $p_T^{\Upsilon(1S)}$ interval agree within the statistical error, which is less

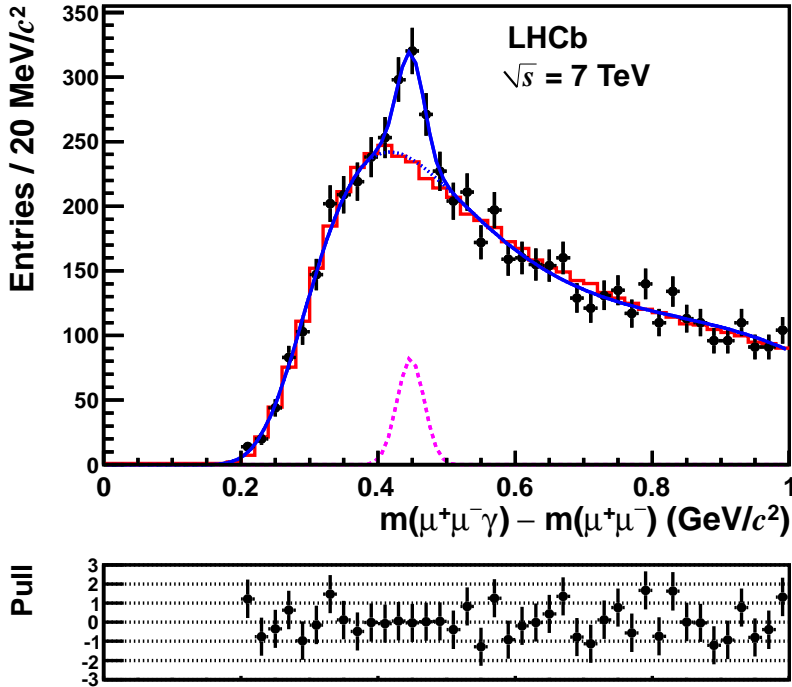


Figure 2: Distribution of the mass difference $m(\mu^+\mu^-\gamma) - m(\mu^+\mu^-)$ for selected $\chi_b(1P)$ candidates (black points), together with the result of the fit (solid blue curve), including background (dotted blue curve) and signal (dashed magenta curve) contributions. The solid (red) histogram is an alternative background estimation using simulated events containing a $\Upsilon(1S)$ that does not originate from a $\chi_b(1P)$ decay, normalized to the data. It is used for evaluation of the systematic uncertainty due to the choice of fitting model. The bottom insert shows the pull distribution of the fit. The pull is defined as the difference between the data and fit value divided by the data error.

than 0.5%.

The conditional $\chi_b(1P)$ reconstruction and selection efficiency is estimated from simulation as

$$\epsilon_{\text{cond}}(\chi_b) = \frac{\epsilon_{\text{tot}}(\chi_b)}{\epsilon_{\text{tot}}(\Upsilon)} = \frac{N_{\text{rec}}^{\text{MC}}(\chi_b)}{N_{\text{gen}}^{\text{MC}}(\chi_b)} \cdot \frac{N_{\text{gen}}^{\text{MC}}(\Upsilon)}{N_{\text{rec}}^{\text{MC}}(\Upsilon)}, \quad (2)$$

where $N_{\text{rec}}^{\text{MC}}(\chi_b)$ and $N_{\text{rec}}^{\text{MC}}(\Upsilon)$ are the number of $\chi_b(1P)$ and $\Upsilon(1S)$ mesons obtained from the fit, and $N_{\text{gen}}^{\text{MC}}(\chi_b)$ and $N_{\text{gen}}^{\text{MC}}(\Upsilon)$ are the number of generated $\chi_b(1P)$ and $\Upsilon(1S)$ mesons, respectively. The value obtained is $\epsilon_{\text{cond}}(\chi_b) = (9.4 \pm 0.1)\%$ for $6 < p_T^{\Upsilon(1S)} < 15 \text{ GeV}/c$ and $2.0 < y^{\Upsilon(1S)} < 4.5$.

The fraction of $\Upsilon(1S)$ originating from $\chi_b(1P)$ decays is determined from the ratio

Table 1: Number of reconstructed $\chi_b(1P)$ and $\Upsilon(1S)$ signal candidates, conditional efficiency and fraction of $\Upsilon(1S)$ originating from $\chi_b(1P)$ decays for different $p_T^{\Upsilon(1S)}$ bins. The uncertainties are statistical only.

$p_T^{\Upsilon(1S)}(\text{GeV}/c)$	6 – 7	7 – 8	8 – 10	10 – 15	6 – 15
$N_{\text{rec}}(\chi_b)$	41 ± 39	35 ± 22	91 ± 30	82 ± 29	201 ± 55
$N_{\text{rec}}(\Upsilon)$	2730 ± 64	2193 ± 57	2866 ± 64	2627 ± 59	$10\,345 \pm 123$
$\epsilon_{\text{cond}}(\chi_b)$ in %	6.7 ± 0.2	8.3 ± 0.2	10.0 ± 0.2	12.8 ± 0.2	9.4 ± 0.1
Fraction in %	23 ± 22	20 ± 12	32 ± 10	25 ± 9	21 ± 6

$$\frac{N_{\text{prod}}(\chi_b)}{N_{\text{prod}}(\Upsilon)} = \frac{N_{\text{rec}}(\chi_b)/\epsilon_{\text{tot}}(\chi_b)}{N_{\text{rec}}(\Upsilon)/\epsilon_{\text{tot}}(\Upsilon)} = \frac{N_{\text{rec}}(\chi_b)/\epsilon_{\text{cond}}(\chi_b)}{N_{\text{rec}}(\Upsilon)}, \quad (3)$$

where $N_{\text{prod}}(\chi_b)$ and $N_{\text{prod}}(\Upsilon)$ are the total numbers of $\chi_b(1P) \rightarrow \Upsilon(1S)\gamma$ and $\Upsilon(1S)$ mesons produced, and $N_{\text{rec}}(\chi_b)$ and $N_{\text{rec}}(\Upsilon)$ are the numbers of reconstructed $\chi_b(1P)$ and $\Upsilon(1S)$ mesons obtained from the fits to the data, respectively. As the muons from the $\Upsilon(1S)$ are explicitly required to trigger the event, the efficiency of the trigger cancels in this ratio. The fraction of $\Upsilon(1S)$ originating from $\chi_b(1P)$ decays for $6 < p_T^{\Upsilon(1S)} < 15 \text{ GeV}/c$ and $2.0 < y^{\Upsilon(1S)} < 4.5$ is found to be $(20.7 \pm 5.7)\%$, where the uncertainty is statistical only.

The procedure is repeated in four bins of $p_T^{\Upsilon(1S)}$, giving the results shown in Table 1 and Fig. 3. No significant $p_T^{\Upsilon(1S)}$ dependence is observed. The mean of the measurements performed in the individual bins is consistent with the measurement obtained in the whole $p_T^{\Upsilon(1S)}$ range.

5 Systematic uncertainties

Studies of quarkonium decays to two muons [3–5, 9, 10] show that the total efficiency depends on the polarization of the vector meson. The effect of the polarization has been studied by repeating the estimation of the efficiencies $\epsilon_{\text{tot}}(\chi_b)$ and $\epsilon_{\text{tot}}(\Upsilon)$ for the extreme $\chi_b(1P)$ and $\Upsilon(1S)$ polarization scenarios and taking the difference in $\epsilon_{\text{cond}}(\chi_b)$ as the systematic uncertainty. The largest variation is found for the cases of 100% transverse and longitudinal polarization of the $\Upsilon(1S)$. We assign this relative variation of $^{+13}_{-26}\%$ as the range due to the unknown polarizations.

The systematic effect due to the unknown $\chi_{bJ}(1P)$, $J = 0, 1, 2$ relative contributions is estimated by varying these fractions in the simulation in such a way that the peak position of the mixture is equal to the peak position observed in the data plus or minus its statistical uncertainty. The maximal relative variation of the result is found to be 7%. This value is taken as a systematic uncertainty due to the unknown $\chi_{bJ}(1P)$ mixture.

The systematic uncertainty due to the photon reconstruction efficiency is determined by comparing the relative yields of the reconstructed $B^+ \rightarrow J/\psi(K^{*+} \rightarrow K^+\pi^0)$ and

Table 2: Relative systematic uncertainties on the fraction of $\Upsilon(1S)$ originating from $\chi_b(1P)$ decays.

Source	Uncertainty (%)
Unknown $\chi_{bJ}(1P)$ mixture	7
Photon reconstruction efficiency	6
Signal and background description	5
Quadratic sum of the above	10

$B^+ \rightarrow J/\psi K^+$ decays in data and simulated events. It is assumed that the reconstruction efficiencies of the two photons from the π^0 are uncorrelated. The uncertainty on the photon reconstruction efficiency is studied as a function of p_T^γ . The largest systematic uncertainty is found to be 6% for photons in the range $0.6 < p_T^\gamma < 0.7 \text{ GeV}/c$, and is dominated by the uncertainties of the B^+ branching fractions.

The systematic uncertainty due to the choice of the background fit model is estimated from simulated events containing an $\Upsilon(1S)$ that does not originate from the decay of a $\chi_b(1P)$. The distribution of the mass difference obtained with these events, using the same reconstruction and selection as for data, is shown in Fig. 2, normalized to the data below $0.38 \text{ GeV}/c^2$. It describes rather well the background contribution above $0.38 \text{ GeV}/c^2$, both in shape and level. The difference between the number of data events and the normalized number of simulated background events in the range $0.38 - 0.50 \text{ GeV}/c^2$ gives an estimate of the signal yield. For $6 < p_T^{\Upsilon(1S)} < 15 \text{ GeV}/c$ the signal yield obtained using this method is 211 to be compared with 201 ± 55 obtained from the fit. The procedure is repeated in each $p_T^{\Upsilon(1S)}$ bin. We also study the variation of signal yield by changing the normalization range to $0.0 - 0.3 \text{ GeV}/c^2$ or $0.7 - 1.0 \text{ GeV}/c^2$. The maximal relative difference of 5% is taken as the uncertainty due to the choice of the signal and background description. Systematic uncertainties are summarized in Table 2.

6 Results and conclusions

The production of $\chi_b(1P)$ mesons is observed using data corresponding to an integrated luminosity of 32 pb^{-1} collected with the LHCb detector in pp collisions at $\sqrt{s} = 7 \text{ TeV}$. The fraction of $\Upsilon(1S)$ originating from $\chi_b(1P)$ decays in the kinematic range $6 < p_T^{\Upsilon(1S)} < 15 \text{ GeV}/c$ and $2.0 < y^{\Upsilon(1S)} < 4.5$ is measured to be

$$(20.7 \pm 5.7 \pm 2.1^{+2.7}_{-5.4})\%,$$

where the first uncertainty is statistical, the second is systematic and the last gives the range of the result due to the unknown polarization of $\Upsilon(1S)$ and $\chi_b(1P)$ mesons.

This result can be compared with the CDF measurement of $(27.1 \pm 6.9 \pm 4.4)\%$ [11], obtained in $p\bar{p}$ collisions at $\sqrt{s} = 1.8 \text{ TeV}$ in the kinematic range $p_T^{\Upsilon(1S)} > 8 \text{ GeV}/c$ and

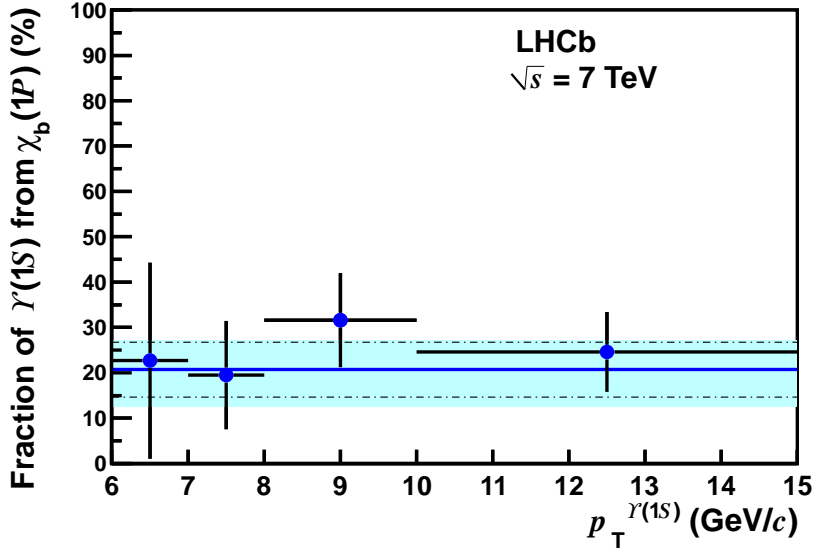


Figure 3: Fraction of $\Upsilon(1S)$ originating from $\chi_b(1P)$ decays for different $p_T^{\Upsilon(1S)}$ bins, assuming production of unpolarized $\Upsilon(1S)$ and $\chi_b(1P)$ mesons, shown with solid circles. The vertical error bars are statistical only. The result determined for the range $6 < p_T < 15 \text{ GeV}/c$ is shown with the horizontal solid line, its statistical uncertainty with the dash-dotted lines, and its total uncertainty (statistical and systematic, including that due to the unknown polarization) with the shaded (light blue) band.

$$|\eta^{\Upsilon(1S)}| < 0.7.$$

The $\chi_b(1P)$ decays are observed to be a significant source of $\Upsilon(1S)$ mesons in pp collisions. This will need to be taken into account in the interpretation of the measured $\Upsilon(1S)$ production cross-section and polarization.

Acknowledgements

We express our gratitude to our colleagues in the CERN accelerator departments for the excellent performance of the LHC. We thank the technical and administrative staff at CERN and at the LHCb institutes, and acknowledge support from the National Agencies: CAPES, CNPq, FAPERJ and FINEP (Brazil); CERN; NSFC (China); CNRS/IN2P3 (France); BMBF, DFG, HGF and MPG (Germany); SFI (Ireland); INFN (Italy); FOM and NWO (The Netherlands); SCSR (Poland); ANCS (Romania); MinES of Russia and Rosatom (Russia); MICINN, XuntaGal and GENCAT (Spain); SNSF and SER (Switzerland); NAS Ukraine (Ukraine); STFC (United Kingdom); NSF (USA). We also acknowledge the support received from the ERC under FP7 and the Region Auvergne.

References

- [1] N. Brambilla *et al.*, *Heavy quarkonium: progress, puzzles, and opportunities*, Eur. Phys. J. **C71** (2011) 1534, [arXiv:1010.5827](#).
- [2] G. T. Bodwin, E. Braaten, and G. P. Lepage, *Rigorous QCD analysis of inclusive annihilation and production of heavy quarkonium*, Phys. Rev. **D51** (1995) 1125, [arXiv:hep-ph/9407339](#), erratum ibid. **D55** (1997) 5853.
- [3] LHCb collaboration, R. Aaij *et al.*, *Measurement of J/ψ production in pp collisions at $\sqrt{s} = 7$ TeV*, Eur. Phys. J. **C71** (2011) 1645, [arXiv:1103.0423](#).
- [4] LHCb collaboration, R. Aaij *et al.*, *Measurement of $\psi(2S)$ meson production in pp collisions at $\sqrt{s} = 7$ TeV*, [arXiv:1204.1258](#), to appear in Eur. Phys. J. C.
- [5] LHCb collaboration, R. Aaij *et al.*, *Measurement of Υ production in pp collisions at $\sqrt{s} = 7$ TeV*, Eur. Phys. J. **C72** (2012) 2025, [arXiv:1202.6579](#).
- [6] CDF collaboration, A. Abulencia *et al.*, *Measurement of $\sigma_{\chi_{c2}} \mathcal{B}(\chi_{c2} \rightarrow J/\psi \gamma) / \sigma_{\chi_{c1}} \mathcal{B}(\chi_{c1} \rightarrow J/\psi \gamma)$ in $p\bar{p}$ collisions at $\sqrt{s} = 1.96$ TeV*, Phys. Rev. Lett. **98** (2007) 232001, [arXiv:hep-ex/0703028](#).
- [7] CDF collaboration, F. Abe *et al.*, *Production of J/ψ mesons from χ_c meson decays in $p\bar{p}$ collisions at $\sqrt{s} = 1.8$ TeV*, Phys. Rev. Lett. **79** (1997) 578.
- [8] HERA-B collaboration, I. Abt *et al.*, *Production of the charmonium states χ_{c1} and χ_{c2} in proton nucleus interactions at $\sqrt{s} = 41.6$ GeV*, Phys. Rev. **D79** (2009) 012001, [arXiv:0807.2167](#).
- [9] LHCb collaboration, R. Aaij *et al.*, *Measurement of the cross-section ratio $\sigma(\chi_{c2}) / \sigma(\chi_{c1})$ for prompt χ_c production at $\sqrt{s} = 7$ TeV*, Phys. Lett. B **714** (2012) 215, [arXiv:1202.1080](#).
- [10] LHCb collaboration, R. Aaij *et al.*, *Measurement of the ratio of prompt χ_c to J/ψ production in pp collisions at $\sqrt{s} = 7$ TeV*, [arXiv:1204.1462](#).
- [11] CDF collaboration, T. Affolder *et al.*, *Production of $\Upsilon(1S)$ mesons from χ_b decays in $p\bar{p}$ collisions at $\sqrt{s} = 1.8$ TeV*, Phys. Rev. Lett. **84** (2000) 2094, [arXiv:hep-ex/9910025](#).
- [12] ATLAS collaboration, G. Aad *et al.*, *Observation of a new χ_b state in radiative transitions to $\Upsilon(1S)$ and $\Upsilon(2S)$ at ATLAS*, Phys. Rev. Lett. **108** (2012) 152001, [arXiv:1112.5154](#).
- [13] D0 collaboration, V. Abazov *et al.*, *Observation of a narrow mass state decaying into $\Upsilon(1S) + \gamma$ in $p\bar{p}$ collisions at $\sqrt{s} = 1.96$ TeV*, [arXiv:1203.6034](#).

- [14] Particle Data Group, J. Beringer *et al.*, *Review of particle physics*, Phys. Rev. **D86** (2012) 010001.
- [15] LHCb collaboration, A. A. Alves Jr. *et al.*, *The LHCb detector at the LHC*, JINST **3** (2008) S08005.
- [16] LHCb collaboration, R. Aaij *et al.*, *Evidence for the decay $B^0 \rightarrow J/\psi\omega$ and measurement of the relative branching fractions of B_s^0 meson decays to $J/\psi\eta$ and $J/\psi\eta'$* , arXiv:1210.2631.
- [17] T. Sjöstrand, S. Mrenna, and P. Skands, *PYTHIA 6.4 physics and manual*, JHEP **05** (2006) 026, arXiv:hep-ph/0603175.
- [18] I. Belyaev *et al.*, *Handling of the generation of primary events in GAUSS, the LHCb simulation framework*, Nuclear Science Symposium Conference Record (NSS/MIC) IEEE (2010) 1155.
- [19] D. J. Lange, *The EvtGen particle decay simulation package*, Nucl. Instrum. Meth. **A462** (2001) 152.
- [20] P. Golonka and Z. Was, *PHOTOS Monte Carlo: a precision tool for QED corrections in Z and W decays*, Eur. Phys. J. **C45** (2006) 97, arXiv:hep-ph/0506026.
- [21] GEANT4 collaboration, J. Allison *et al.*, *Geant4 developments and applications*, IEEE Trans. Nucl. Sci. **53** (2006) 270; GEANT4 collaboration, S. Agostinelli *et al.*, *GEANT4: A simulation toolkit*, Nucl. Instrum. Meth. **A506** (2003) 250.
- [22] M. Clemencic *et al.*, *The LHCb simulation application, GAUSS: design, evolution and experience*, J. of Phys. : Conf. Ser. **331** (2011) 032023.
- [23] T. Skwarnicki, *A study of the radiative cascade transitions between the Upsilon-prime and Upsilon resonances*, PhD thesis, Institute of Nuclear Physics, Krakow, 1986, DESY-F31-86-02.